"Physics of Auroral Phenomena", Proc. XXI Annual Seminar, Apatity, pp.87-90, 1998

Polar Geophysical Institute

INFLUENCE OF STORMS ON THE MAGNETOSPHERIC MAGNETIC FIELD

A.A.Ostapenko, Yu.P.Maltsev *(Polar Geophysical Institute, Apatity, Russia)*

Abstract. We used the database of *Fairfield et al.* [1994] for studying response of the magnetic field at distances of 10 $R_E > x > -30\ R_E$ to changes in the *Dst* index. An enhancement of the storm time depression results in increasing of both the cross-tail and ring currents, the former effect being predominant.

Introduction

Magnetic storms are accompanied by pronounced variations of the magnetic field in the magnetosphere. These variations were studied in some local magnetospheric regions. *Sugiura* [1973], *Fairfield et al.* [1987], *Iijima et al.* [1990] examined the responses of the field at distances from 2 to 8 R_E near the equatorial plane to changes in the *Kp* and *Dst* indices. *Fairfield* [1986], *Boumjohann et al.* [1990], *Nakai et al.* [1991], *Fairfield and Jones* [1996], *Kokubun et al.* [1996], *Ho and Tsurutani* [1997] investigated the field variability in the magnetotail.

The response of the entire magnetosphere to storms has not been obtained yet. The aim of this paper is to find the pattern of the differential magnetic response at distances 10 $R_E > x > -30\ R_E$, 15 $R_E > y > -15\ R_E$, 15 $R_E > z > -15\ R_E$ to changes in the *Dst* index.

Data processing technique

We have used the database of *Fairfield et al.* [1994]. It includes 68,000 three-component magnetic field measurements obtained by 11 satellites at distances 10 $R_E > x > -40\ R_E$, $|y| < 20\ R_E$, $|z| < 20\ R_E$. Hourly *Dst* and three-hourly *Kp* indices have been available for all the measurements. Hourly values of the solar wind dynamic pressure *p* and three components of the interplanetary magnetic field (IMF) have been known for most of the measurements. Hourly values of the *AE* index have been available for 47 per cent of the measurements.

The database was divided into three subsets differing by values of the *Dst* index. Table 1 shows the number of measurements *N* as well as average values of *Dst, Kp, AE, p*, and IMF B_z for each subset. The external magnetic field of each subset was averaged in cubic bins with the edge of 4 R_E.

Table 1. Average parameters of three subsets differing by the levels of the storm activity

Conditions	Subset	*N*	*Dst*, nT	*Kp*	*AE*, nT	*p*, nPa	*IMFz*, nT
Quiet	*Dst* > 0 nT	15465	7	1.5	99	2.4	1.2
Weak storm	0 > *Dst* > -50 nT	47952	-18	2.3	207	2.0	-0.1
Strong storm	*Dst* < -50 nT	4640	-74	4.3	445	3.4	-2.2

To examine the pure magnetic response to the *Dst* index we divided the whole data set into two equal subsets differing by the magnitude of this index only, the other parameters being invariable. Average values of *Dst, Kp, p*, and IMF B_z for each subset are shown in Table 2. The *AE* index was not taken into consideration because of comparatively small amount of its data available. The response was determined as the difference of magnetic fields of the two subsets.

Table 2. Average parameters of two subsets used for studying the pure response to *Dst* change.

Subset	*Dst*, nT	*Kp*	*p*, nPa	*IMFz*, nT
Dst < -16 nT	-4	2.24	2.23	0.01
Dst > -16 nT	-31	2.21	2.23	0.05

In order to improve the spatial resolution near the magnetotail neutral sheet which position z_{ns} suffers strong variations related to the Earth dipole tilt [*Fairfield*, 1986] we introduced the coordinate $z' = z - z_{ns}$ where *z* is the GSM coordinate. The dawn-dusk and north-south symmetry was assumed.

Results

Figure 1 shows the magnetic field $\mathbf{B}^{ext}$ of the external sources in the noon-midnight meridian plane under three levels of the storm activity: $Dst > 0$, $0 > Dst > -50$ nT, and $Dst < -50$ nT. Figure 2 shows the contours B_z^{ext} = const in the equatorial plane ($z = 0$). Figures 3, 4, and 5 show the contours B_x^{ext} = const in the planes $x = -20\ R_E$, $x = -10\ R_E$, and x=0, respectively. Figure 6 shows the magnetospheric response to the change of the *Dst* index, the other parameters keeping invariable. For calculating the response we subtracted the field of the *Dst* > -16 nT subset from the field of the subset with *Dst* < -16 nT (Table 2).

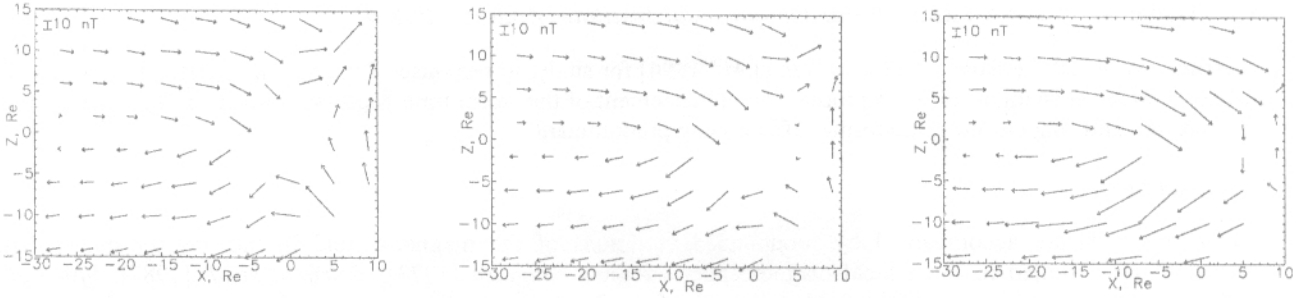

Dst > 0 -50 nT < *Dst* < 0 *Dst* < -50 nT

Figure 1. The magnetic field of external sources in the noon-midnight meridian plane under three levels of the storm activity: *Dst* > 0 (the left panel),) 0 > *Dst* > -50 nT (the middle panel), and *Dst* < -50 nT (the right panel).

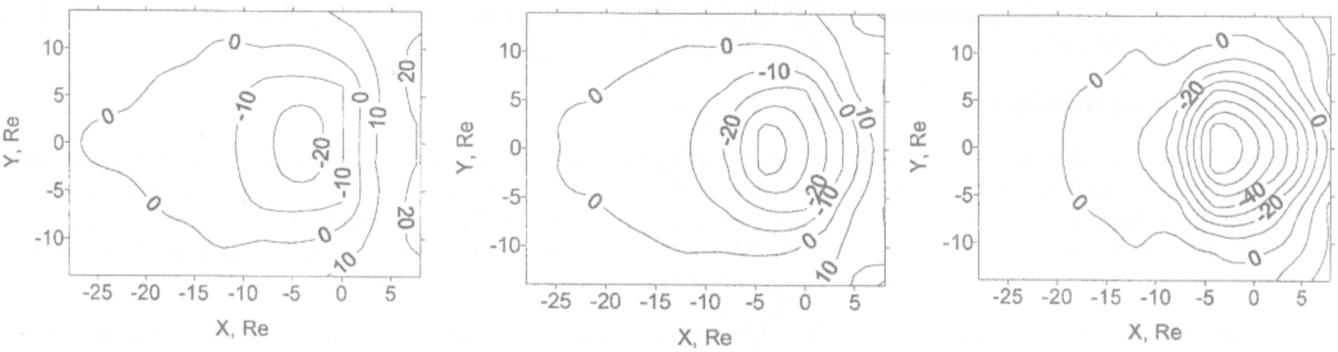

Dst > 0 -50 nT < *Dst* < 0 *Dst* < -50 nT

Figure 2. Contours B_z^{ext} = const (in nT) in the equatorial plane.

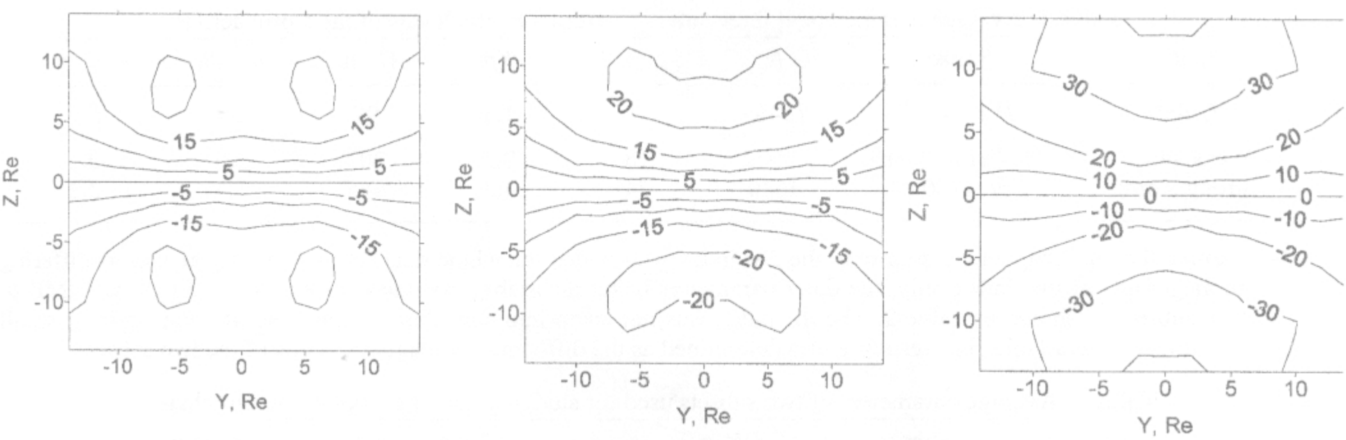

Dst > 0 -50 nT < *Dst* < 0 *Dst* < -50 nT

Figure 3. Contours B_x^{ext} = const (in nT) in the plane $x = -20\ R_E$.

Discussion

In Figure 1 the dominant effect of the magnetotail current is well pronounced under all levels of storm activity. One can see from Figures 3 and 4 that the magnetic field in the tail lobes grows when the storm time depression increases, which evidences the intensification of the cross-tail current. *Boumjohann et al.* [1990] have found such a growth with increasing *AE* index. *Nakai et al.* [1991] as well as *Fairfield and Jones* [1996] – with growing solar wind dynamic pressure and southward IMF. *Kokubun et al.* [1996], and *Ho and Tsurutani* [1997] observed the strong field in the distant tail lobe during the main stage of storms. Figure 5 shows that the most significant growth of B_x occurs in the near-Earth lobes, at $x = 0$. This is probably caused by intensification of the region 1 Birkeland currents during storms.

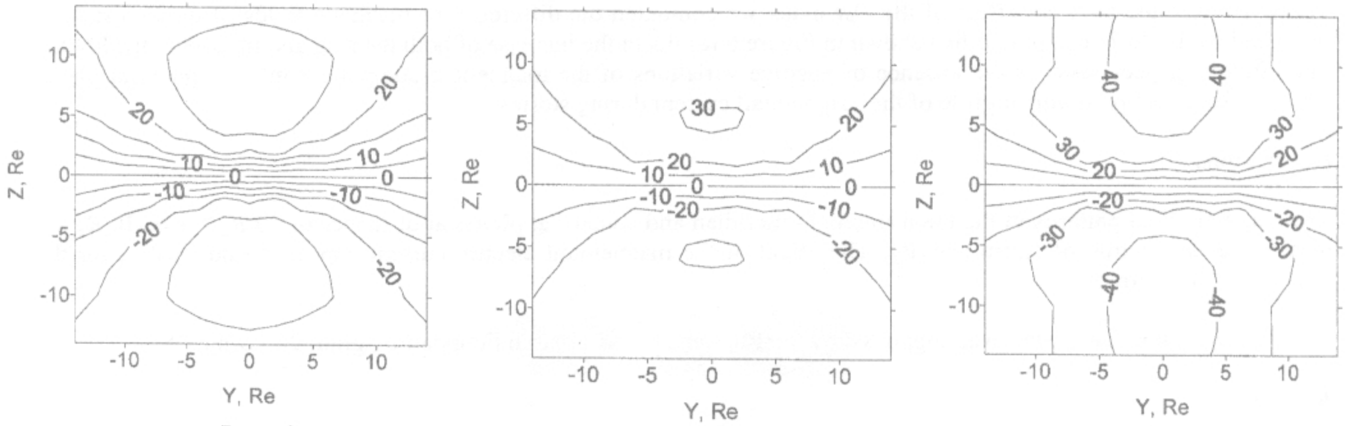

Dst > 0 | -50 nT < *Dst* < 0 | *Dst* < -50 nT

Figure 4. Contours B_x^{ext} = const (in nT) in the plane x = -10 R_E.

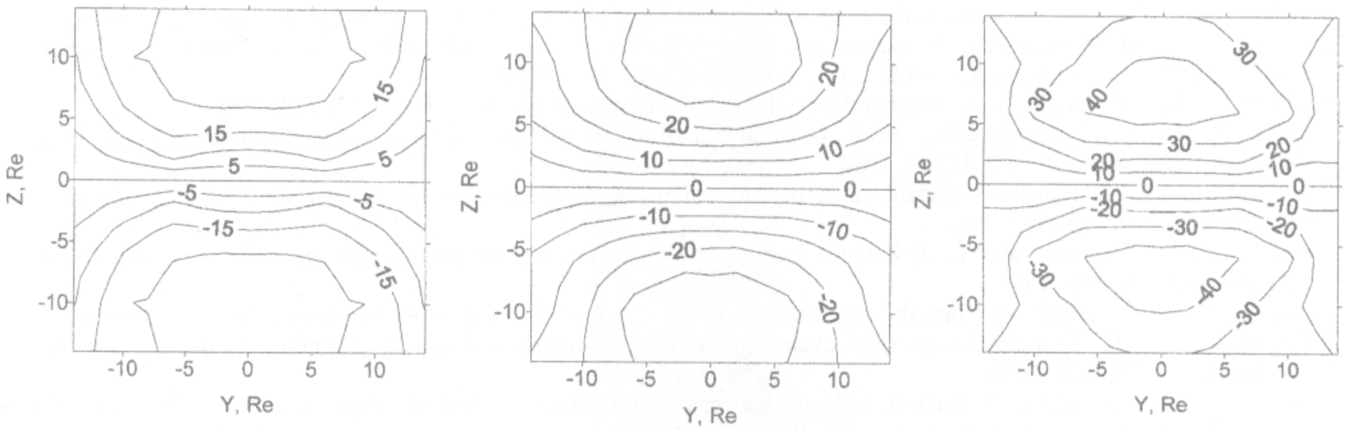

Dst > 0 | -50 nT < *Dst* < 0 | *Dst* < -50 nT

Figure 5. Contours B_x^{ext} = const (in nT) in the plane x = 0.

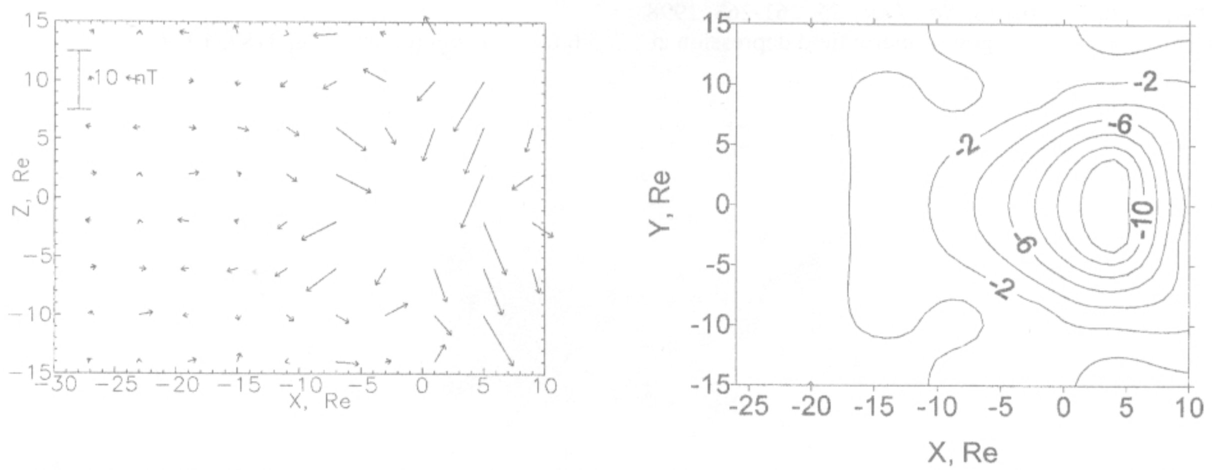

Figure 6. The magnetic response to ΔDst = -27 nT, the other parameters (*Kp*, *p*, and *IMFz*) keep invariable. The left panel corresponds to the noon-midnight meridian plane, the right panel – to the equatorial plane.

Figure 2 shows the depression of the external magnetic field in the equatorial plane of the magnetosphere growing with increasing storm activity. Under quiet conditions the depression takes place in the night side. During storms the depression grows and extends for the entire equatorial magnetosphere. Such a growth in the inner region (r < 8 R_E) was noticed earlier by *Sugiura* [1973], *Fairfield et al.* [1987], *Iijima et al.* [1990], *Ostapenko and Maltsev* [1997].

Strong storms are usually accompanied by enhancement of the solar wind dynamic pressure p (Table 1). The increase in p causes the growth of the magnetotail current [*Nakai et al.*, 1991; *Fairfield and Jones*,1996; *Ostapenko and Maltsev*, 1998]. To examine the pure effect of the *Dst* index we computed the difference of magnetic fields of the two subsets described by Table 2. The pure effect shown in Figure 6 results in the increase of both the ring and magnetotail currents. The interesting peculiarity is the absence of positive variations of the magnetic z-component in the equatorial plane. This evidences the predominant role of the magnetotail current during storms.

Conclusions

The magnetic field patterns in the noon-midnight meridian and equatorial planes at distances of 10 $R_E > x > -30\ R_E$ are obtained as a function of storm activity. The effect of the magnetotail electric current appears to dominate over the effects of other currents.

Acknowledgments. This work was supported by the Russian Basic Research Foundation, grant 96-05-64305.

References

Baumjohann, W., G. Paschmann, and H. Lühr, Pressure balance between lobe and plasma sheet, *Geophys. Res. Lett.*, *17*, 45, 1990.

Fairfield, D. H., The magnetic field of the equatorial magnetotail from 10 to 40 Re, *J. Geophys. Res.*, *91*, 4238, 1986.

Fairfield, D. H., M. H. Acuna, L. J. Zanetti, and T. A. Potemra , The magnetic field of the equatorial magnetotail: AMPTE/CCE observations at $R < 8.8\ R_E$, *J. Geophys. Res.*, *92*, 7432, 1987.

Fairfield, D. H., and J. Jones, Variability of the tail lobe field strength, *J. Geophys. Res.*, *101*, 7785, 1996.

Fairfield, D. H., N. A. Tsyganenko, A. V. Usmanov, and M. V. Malkov, A large magnetosphere magnetic field database, *J. Geophys. Res.*, *99*, 11319, 1994.

Ho, C. M., and B. T. Tsurutani, Distant tail behavior during high speed solar wind streams and magnetic storms, *J. Geophys. Res.*, *102*, 14165, 1997.

Iijima, T., T. A. Potemra, and L. J. Zanetti, Large-scale characteristics of magnetospheric equatorial currents, *J. Geophys. Res.*, *95*, 991, 1990.

Kokubun, S., L. A. Frank, K. Hayashi, Y. Kamide, R. P. Lepping, T. Mukai, R. Nakamura, W. R. Paterson, T. Yamamoto, and K. Yumoto, Large field events in the distant magnetotail during magnetic storms, *J. Geomag. Geoelectr.*, *48*, 561-575, 1996.

Nakai, H., Y. Kamide, and C. T. Russell, Influences of solar wind parameters and geomagnetic activity on the tail lobe magnetic field: a statistical study, *J. Geophys. Res.*, *96*, 5511, 1991.

Ostapenko, A. A., and Y. P. Maltsev, Relation of the magnetic field in the magnetosphere to the geomagnetic and solar wind activity, *J. Geophys. Res.*, *102*, 17467, 1997.

Ostapenko, A. A., and Yu. P. Maltsev, Three-dimensional magnetospheric response to variations in the solar wind dynamic pressure, *Geophys. Res. Lett.*, *25*, 261-263, 1998.

Sugiura, M., Quiet time magnetospheric field depression at 2.3-3.6 R_E , *J. Geophys. Res.*, *78*, 3182, 1973.